Available online www.jocpr.com

Journal of Chemical and Pharmaceutical Research, 2014, 6(3):717-722

Research Article

ISSN : 0975-7384
CODEN(USA) : JCPRC5

Prediction method for temperature distribution in reduction section of gas-based direct reduced iron shaft furnace

Junli Ge[a], Minghua Bai[a], Hongliang Zhou[b], Jian Wang[a] and Yingmin Piao[a]

[a]*National Engieering Research Center for Equipment and Technology of Cold Strip Rolling, Yanshan University, Qin Huangdao, Hebei, China*
[b]*School of Mechanics and Power Engineering, Henan Polytechnic University , Jiaozuo, Henan, China*

ABSTRACT

Temperature distribution plays a crucial role in the process of direct reduced iron (DRI) production. Based on Baogang and Lunan (BL) semi-industrial equipment and process parameters, a gas-solid heat transfer model is established to study the temperature field in the reduction section of gas-based DRI shaft furnace. In the case of different reduction gas quantities in reduction section of DRI shaft furnace, iron ore pellets are simplified as porous media for the convenience of temperature field analysis with consideration of chemical reaction heat. The numerical results show that the thermal efficiency of the reduction gas decreases with the increasing of the reduction gas quantity, but the DRI shaft furnace top gas temperature increases. Meanwhile the numerical results have a good agreement with BL experimental ones, which indicates that the simplified gas-solid heat transfer model can be used to predict the temperature distribution effectively in reduction section of gas-based DRI shaft furnace.

Key words: Gas-based DRI shaft furnace; Baogang and Lunan; Gas-solid heat transfer; Chemical reaction heat; Thermal efficiency

INTRODUCTION

Gas-based direct reduced iron (DRI) shaft furnace is a closed countercurrent reactor, where the iron ore pellets fed at the top of the shaft furnace fall from top to bottom and the high temperature reduction gas flows from bottom to top. In the reduction section of gas-based DRI shaft furnace, complex physical and chemical reactions occur between high temperature reduction gas and low temperature ore pellets, which lead to heat transfer between them and precipitation of elemental iron. In this process, temperature field and reduction gas quantity both have important effects not only on reduction reaction rate, reduction swelling ratio and reduction gas utilization ratio in DRI shaft furnace, but also on structure design of the furnace [1].

Hui Xu, professor of Northeastern university has built a one-dimensional mathematical model, which is used to study the DRI production process based on the equipment and process parameters of MIDREX shaft furnace [2]. In this work, on the basis of Baogang and Lunan (BL) semi-industrial equipment and process parameters [3-5], the temperature field and gas composition for different reduction gas quantities in reduction section of DRI shaft furnace are analyzed by finite element method with the consideration of the chemical reaction heat, which makes the advantage of DRI method more noticeable [6].

GAS-SOLID HEAT TRANSFER MODEL OF DRI SHAFT FURNACE

The DRI shaft furnace can be seen as a two-dimensional axisymmetric structure model in order to simplify the calculation, and the basic assumptions are as follows:
(1) Iron ore pellets are considered as homogeneous porous media, which fall down at an even speed in DRI shaft furnace;

(2) Mass transfer process is negligible in DRI shaft furnace, and chemical reaction heat is included in the energy equation;
(3) Physical parameters changes of iron ore pellets and reduction gas due to the temperature in DRI shaft furnace are also negligible;
(4) Considering the chemistry reaction heat, one-step reaction method is chosen for the convenience of numerical calculation.

1. Geometrical model

Fig. 1 shows the geometrical model of DRI shaft furnace, and its main operation parameters are listed in Table 1.

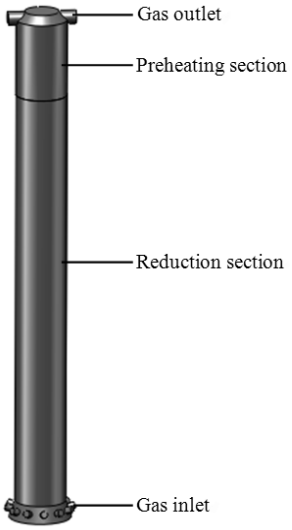

Fig. 1 Geometrical model of DRI shaft furnace

Table 1.Main operation parameters of DRI shaft furnace

Height of reduction section (mm)	4000	Production of iron (t/d)	5
Diameter of reduction section (mm)	300	Density of iron ore pellet (Kg/m3)	2300
Utilization coefficient in reduction section (t/(d□m3))	4.8	Porosity	0.3

2. Boundary conditions

2.1 Boundary conditions of DRI shaft furnace walls

DRI shaft furnace walls are considered to be no slip, and convective heat transfer boundary condition between shaft furnace walls and reducing gas is given by:

$$Q = h_w(T_w - T_g) \tag{1}$$

when the heat losses of DRI shaft furnace walls are negligible, Q=0.

2.2 Boundary conditions at gas inlet

Reducing gas is composed of 60% H_2 and 40% CO with its temperature 1173 K, whose velocity is determined by different reduction gas quantities.

2.3 Boundary conditions at gas outlet

DRI shaft furnace top gas pressure is 150 kPa, and its temperature is assumed to be 300 K, which equals to original iron ore pellets temperature.

2.4 Symmetric boundary conditions

Considering the axial symmetry of DRI shaft furnace model, next equation is obtained:

$$\begin{cases} \dfrac{\partial u}{\partial x} = 0 \\ \dfrac{\partial T_s}{\partial x} = \dfrac{\partial T_g}{\partial x} = 0 \end{cases} \tag{2}$$

2.5 Computational domain boundary conditions
Boundaries of the computational domain are considered to be sliding meshes with the sliding velocity 0.00022 m/s, which refers to the falling speed of iron ore pellets.

3 Key parameters
3.1 Inertial resistance coefficient and viscous resistance coefficient
Porous media mode is chosen to deal with the numerical simulation of gas-solid heat transfer in DRI shaft furnace, and its momentum equation includes an additional momentum source S_i, which is composed of two terms, one is viscous loss, the other is internal resistance loss [7,8]:

$$S_i = \sum_{j=1}^{3} D_{ij}\mu v_j + \sum_{j=1}^{3} C_{ij}\frac{1}{2}\rho|v_j|v_j \tag{3}$$

where D_{ij} is the viscous resistance coefficient with a value 1.52×10^8 m^{-2}; C_{ij} is viscous resistance coefficient with a value 16963 m^{-1} [9].

3.2 Effective heat transfer coefficient in porous media
Effective heat transfer coefficient K in the porous media model can be written as:

$$K = \phi K_f + (1-\phi)K_s \tag{4}$$

where ϕ is the porosity with a value 0.3; K_f is the heat transfer coefficient of fluid; K_s is the heat transfer coefficient of solid.

3.3 Thermal efficiency coefficient
Thermal efficiency can be expressed as:

$$\eta = \frac{A}{B} = 1 - \frac{C}{B} \tag{5}$$

where A is the heat absorbed by iron ore pellets, B is total heat of reducing gas, C is the heat taken away by DRI shaft furnace top gas.

3.4 Chemistry reaction heat
Complex physical and chemical reactions occur in DRI shaft furnace, and the needed energy is supplied by the high temperature reducing gas. In this model, each reduction reaction heat can be seen as source term form, which is added to heat transfer equation of iron ore pellets, and one-step reaction method is chosen to simplify the numerical calculation. The reduction reaction equations are described as [10]:

$$\frac{1}{2}Fe_2O_3 + \frac{3}{2}CO = Fe + \frac{3}{2}CO_2 \quad \Delta H = -16.62\ KJ/mol \tag{6}$$

$$\frac{1}{2}Fe_2O_3 + \frac{3}{2}H_2 = Fe + \frac{3}{2}H_2O \quad \Delta H = +45.57\ KJ/mol \tag{7}$$

Reaction heat is regarded as an energy source, which is given as [11-13]:

$$S_h = -Fe\sum_{Fe}\left(\frac{h_{Fe}^0}{M_{Fe}} + \int_{ref,Fe}^{T} C_{p,Fe}dT\right)R_{Fe} \tag{8}$$

where h_{Fe}^0 is the formation enthalpy of Fe; R_{Fe} is the volumetric heat release rate of Fe.

RESULTS AND DISCUSSION

1 Temperature changes in reduction section of DRI shaft furnace
The falling speed of iron ore pellets is 0.00022 m/s in DRI shaft furnace and the reduction gas quantity is 1445 Nm^3/t with its temperature 1173 K. Fig. 2 shows the temperature change curves of reduction section at different times. It can be found that because of the gas-solid heat transfer, half of the iron ore pellets are heated to 500 K

above after an hour, a quarter of which are heated to 900 K. Two hours later, three quarters of the iron ore pellets are heated to 900 K, half of which are heated to 1173 K, and after three hours the temperature field of reduction section reaches its steady state.

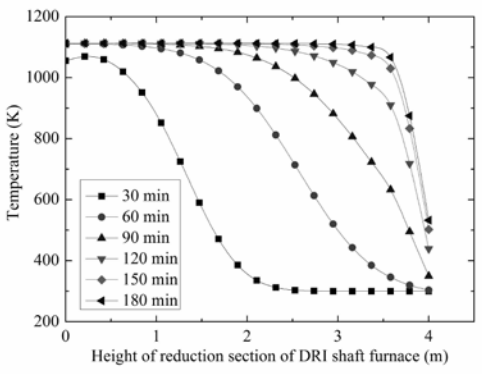

Fig. 2 Temperature change curves of reduction section at different times

Fig. 3 shows the reaction heat curves for different positions of DRI shaft furnace after 2700 s. It can be seen that, because of the uneven gas flow distribution, the energy absorption capability of reduction reaction becomes stronger and stronger from the axis to edge of DRI shaft furnace, which indicates that the reaction rate becomes faster and faster in the same direction.

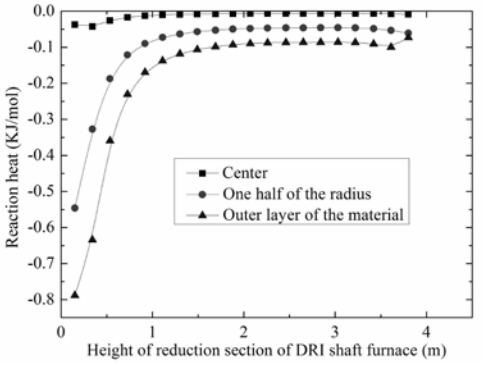

Fig. 3 Reaction heat curves for different positions of DRI shaft furnace after 2700 s

2 Effects of different reduction gas quantities on temperature field in reduction section

Fig. 4 shows the temperature change curves for different reduction gas quantities after 2.5 hours. It is found that the larger the reduction gas quantity the higher the temperature at the same height in reduction section, which means that the larger the reduction gas quantity the faster the preheating rate of iron ore pellets at the same time. The iron ore pellets in 5 meters from the gas outlet are heated to 1173 K after 40 minutes when the reduction gas quantity is 1700 Nm^3/t. While it takes a long time to for the iron ore pellets to be heated to specified temperature as the reduction gas quantity decreases, and when the reduction gas quantity is 1223 Nm^3/t, it takes 110 minutes for the iron ore pellets to be wholly heated.

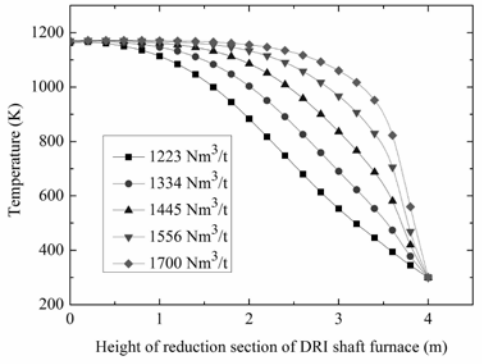

Fig. 4 Temperature change curves for different reduction gas quantities after 2.5 h

Fig. 5 shows the temperature change curves for different reduction gas quantities in steady state. It can be seen that the temperature of most iron ore pellets is consistent with that of reduction gas at the gas inlet of DRI shaft furnace, and temperature gradient only exists in the range of 0~1 meter from the gas outlet, whose range becomes narrower with the increasing of the reduction gas quantity.

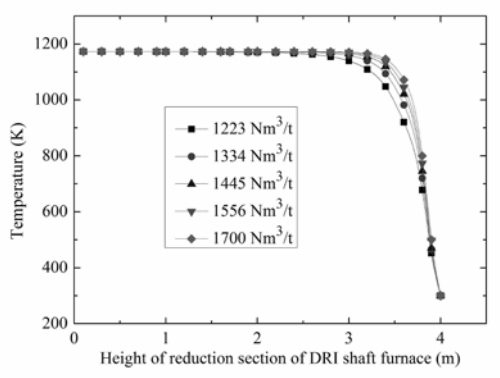

Fig. 5 Temperature change curves for different reduction gas quantities in steady state

3 Effects of different gas compositions on temperature field in reduction section

Temperature change curves for three kinds of gas compositions (pure hydrogen, pure carbon monoxide, 60% hydrogen +40% carbon monoxide) in steady state are shown in Fig. 6. It can be found that when the pellets are reduced with carbon monoxide, the reduction reaction is exothermic, which makes partial material temperature higher than 1173K. Whereas when pure hydrogen is chosen as the reduction gas, the reduction reaction is endothermic, which makes partial material temperature lower than 1173 K. Too high temperature can melt the iron ore pellets, which is bad for the pellets drop, while low temperature has a bad effect on the reduction reaction, which is harmful for quality of reduced iron. So a proper proportion of reduction gas is needed to enhance the efficiency of reduction reaction.

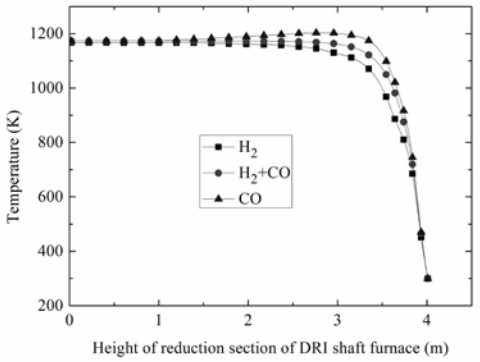

Fig. 6 Temperature change curves for different reduction gas compositions

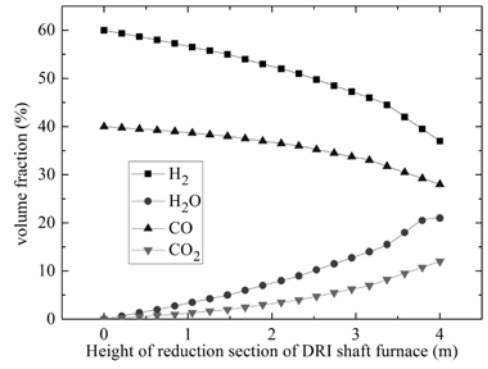

Fig. 7 Reducing gas compositions change curves in reduction section

4 Thermal efficiency analysis in reduction section

Fig.7 shows the reducing gas compositions change curves in reduction section. It can be seen that hydrogen content and carbon monoxide content decrease with the increasing of height in reduction section, but the water vapor content and carbon dioxide content increase. In the range of 0.5~1 meter from the gas outlet, the decreasing rates of hydrogen content and carbon monoxide content and the increasing rates of water vapor content and carbon dioxide content are the fastest, which means that there is a most intense reduction reaction here. Table 2 lists the values of thermal efficiency for different reduction gas quantities. It can be seen that values of thermal efficiency in reduction section decrease with the increasing of reduction gas quantities.

Table 2. Values of thermal efficiency for different reduction gas quantities

Reduction gas compositions (%)			60%H_2+40%CO		
Initial temperature of reduction gas (K)			1173		
Reduction gas quantities (Nm^3/t)	1223	1334	1445	1556	1700
Temperature of DRI shaft furnace top gas (K)	633.868	666.822	701.986	742.236	780.668
Heat taken away by DRI shaft furnace top gas (KJ)	1337851.076	1481452.441	1640755.892	1790074.512	1972694.191
Total heat of reducing gas (KJ)	2033208.323	2217743.175	2402278.026	2586812.878	2826209.443
Thermal efficiency	0.342	0.332	0.317	0.308	0.302

5 Results comparison between numerical simulation and BL test

Table 3 shows the results comparison between numerical simulation and BL test about DRI shaft furnace top gas compositions and reduction gas consumption, when reduction gas quantity is 1556 Nm^3/t with its initial temperature 1173 K, and DRI shaft furnace top gas pressure is 150 kPa. It can be found that there is very good agreement between the numerical results and BL ones, which means that the geometrical model can simulate the reduction reaction well in reduction section of DRI shaft furnace.

Table 3. Results comparison between numerical simulation and BL test

Basic parameters		Numerical results	BL results
DRI shaft furnace top gas compositions (%)	Hydrogen	33.8	31.3
	Water vapor	26.2	28.7
	Carbon monoxide	26.5	25.1
	Carbon dioxide	13.5	14.9
Reduction gas consumption (Nm^3/t)		610	679

CONCLUSION

(1) Reduction gas quantity has a significant effect on the time for the temperature field of DRI shaft furnace to reach the steady state, the larger the reduction gas quantity the shorter the time.

(2) An appropriate reduction gas quantity can improve the thermal efficiency, the smaller the reduction gas quantity the higher the thermal efficiency. The thermal efficiency is highest with its value 0.342 when the reduction gas quantity is 1223 Nm^3/t.

(3) The numerical results show good agreement with BL ones, which indicates that the temperature distribution in reduction section of DRI shaft furnace can be effectively predicted by the simplified gas-solid heat transfer model.

REFERENCES

[1] Li YQ, Chen H, Zhou YS. *Special Steel* **1999**; 22: 40-43.
[2] Xu H, Zou ZS, Zhou YS. *Journal of Materials and Metallurgy* **2009**; 8: 7-11.
[3] Li YQ, Chen H, Li XW. *Bao Steel Technology* **2000**; 5: 21-24.
[4] Chen H, Li YQ, Zhou YS. BL *Bao Steel Technology* **1999**; 4: 25-28.
[5] Li YQ, Chen H, Zhou YS. *Iron Steel* **1999**; 34: 6-10.
[6] Zafar HK, Pritchard D. *International Journal of Heat and Mass Transfer* **2013**; 61: 1-17.
[7] Chang J, Yang SQ, Zhang K. *Chemical Engineering Research and Design* **2011**; 89: 894–903.
[8] Broqueville AD, Wilde JD. *Chemical Engineering Science* **2009**; 64: 1232-1248.
[9] Ge JL, Bai MH, Piao YM. *Iron and Steel* **2014**; 49: 11-16.
[10] Li J, Yu MY, Zhou GF. *Journal of Wuhan University of Science and Technology* **1996**; 19: 282-288
[11] Chang J, Wang G, Gao JS. *Powder Technology* **2012**; 217: 50-60.
[12] Azoumah Y, Mazet N, Neveu P. *International Journal of Heat and Mass Transfer* **2004**; 47: 2961–2970.
[13] Hiroyuki M, Hideyuki O, Masaki A. *Powder Technology* **2012**; 231: 7–17.